Distinct Principal Modes of Early and Late Summer Rainfall Anomalies in East Asia*

BIN WANG

Department of Meteorology and International Pacific Research Center, University of Hawaii at Manoa, Honolulu, Hawaii

JIAN LIU

Nanjing Institute of Geography and Limnology, Chinese Academy of Sciences, Nanjing, China

JING YANG

State Key Laboratory of Earth Surface Processes and Resource Ecology, Beijing Normal University, Beijing, China

TIANJUN ZHOU

State Key Laboratory of Numerical Modeling for Atmospheric Sciences and Geophysical Fluid Dynamics, Institute of Atmospheric Physics, Chinese Academy of Sciences, Beijing, China

ZHIWEI WU

Department of Meteorology and International Pacific Research Center, University of Hawaii at Manoa, Honolulu, Hawaii

(Manuscript received 22 September 2008, in final form 22 January 2009)

ABSTRACT

The current seasonal prediction of East Asia (EA) summer monsoon deals with June–July–August (JJA) mean anomalies. This study shows that the EA summer monsoon may be divided into early summer [May–June (MJ)] and late summer [July–August (JA)] and exhibits remarkable differences in mean state between MJ and JA. This study reveals that the principal modes of interannual precipitation variability have distinct spatial and temporal structures during the early and late summer. These principal modes can be categorized as either El Niño–Southern Oscillation (ENSO) related or non-ENSO related. During the period of 1979–2007, ENSO-related modes explain 35% of MJ variance and 45% of JA variance, and non-ENSO-related modes account for 25% of MJ variance and 20% of JA variance. For ENSO-related variance, about two-thirds are associated with ENSO decaying phases, and one-third is associated with ENSO developing phases. The ENSO-related MJ modes generally concur with rapid decay or early development of ENSO episodes, and the opposite tends to apply to ENSO-related JA modes. The non-ENSO MJ mode is preceded by anomalous land surface temperatures over southern China during the previous March and April. The non-ENSO JA mode is preceded by lasting equatorial western Pacific (the Niño-4 region) warming from the previous winter through late summer. The results suggest that 1) prediction of bimonthly (MJ) and (JA) anomalies may be useful, 2) accurate prediction of the detailed evolution of ENSO is critical for prediction of ENSO-related bimonthly rainfall anomalies over East Asia, and 3) non-ENSO-related modes are of paramount importance during ENSO neutral years. Further establishment of the physical linkages between the non-ENSO modes and their corresponding precursors may provide additional sources for EA summer monsoon prediction.

1. Introduction

The seasonal prediction of summer rainfall over East Asia (EA) has been a great challenge. State-of-the-art multimodel ensemble prediction of summer precipitation in subtropical–extratropical EA (20°–50°N, 100°–130°E) has shown moderate prediction skills: 14 dynamic models that participated in a 24-yr (1981–2004) hindcast experiment show a correlation skill score between

* School of Ocean and Earth Science and Technology Contribution Number 7639 and International Pacific Research Center Contribution Number 589.

Corresponding author address: Bin Wang, International Pacific Research Center, School of Ocean and Earth Science and Technology, University of Hawaii at Manoa, 1680 East West Road, Post 401, Honolulu, HI 96822.
E-mail: wangbin@hawaii.edu

DOI: 10.1175/2009JCLI2850.1

0.1 and 0.25 (Wang et al. 2008a). Why are the dynamical model's prediction skills so low in this subtropical–extratropical region? Is this due to lack of inherent predictability? Or is it due to deficiencies in the current climate prediction systems? The present study aims to elaborate on the sources of variability and predictability regarding EA summer precipitation.

The rainy season over EA experiences the most spectacular northward march on earth during the period from May to August. The EA monsoon's rain advances from 15°N in May all the way to 45°N by early August. In early May, the summer rainy season starts over the Indochina Peninsula (Matsumoto and Murakami 2002) and southern China (Ding and Sikka 2006) and by mid-May over the South China Sea (Tao and Chen 1987). The rainy season generally retreats toward the end of August except for a restricted region in northwestern central China and northern Japan (e.g., Wang and LinHo 2002). Thus, May through August is the primary rainy season over EA.

As will be shown in section 3, the East Asian summer monsoon (EASM) can be divided into two subseasons: early summer [May and June (MJ)] and late summer [July and August (JA)]; furthermore, there are pronounced differences in the subseasonal mean states between MJ and JA. Previous studies have found significantly different patterns of interdecadal rainfall changes at early summer and late summer (Xin et al. 2006; Yu and Zhou 2007). El Niño–Southern Oscillation (ENSO) has long been recognized as a major cause of variability in EASM rainfall (e.g., Tu 1955; Fu and Teng 1988; Lau and Nath 2000; Wang et al. 2008b; and many others). The pronounced differences in mean state between MJ and JA are expected to have a significant impact on the anomalous monsoon response to remote ENSO forcing, even when the forcing is the same. Additionally, the majority of ENSO events mature in the boreal winter, and the way in which ENSO affects the EA summer rainfall depends on its phase of evolution (e.g., Fu and Teng 1988; Huang and Wu 1989). Since each ENSO event evolves differently, especially its timing of development and decay (according to calendar month), ENSO's influences on the EASM might significantly differ between MJ and JA.

The possibilities outlined in the previous paragraph motivated us to examine the differences between MJ and JA in interannual variation of precipitation. We will show in section 4 that the principal modes of interannual precipitation variability during early summer (MJ) and late summer (JA) indeed exhibit different behavior. In sections 5 through 7, we will further address the following questions: Does ENSO affect early and late summer precipitation differently? How does the seasonal march of the mean state modulate interannual variation in precipitation? Are there any other factors besides ENSO that influence MJ or JA variability? If so, what are they? The last section presents a summary and discussion.

2. Data and method

The data we used comprise the Climate Prediction Center Merged Analysis of Precipitation (CMAP) dataset (Xie and Arkin 1997), the improved extended reconstructed SST version 2 (ERSSTv2) data (Smith and Reynolds 2004), and the circulation fields derived from the National Centers for Environmental Prediction/Department of Energy (NCEP/DOE) reanalysis 2 (Kanamitsu et al. 2002). Land surface temperature data were obtained from the Climate Research Unit (CRU; Jones et al. 1999), which provides information from 4000 weather stations distributed around the world. To focus on interannual variation, a Fourier harmonic bandpass filter of 2–8 yr was used to isolate signals of interannual variation.

Empirical orthogonal function (EOF) analysis of the bimonthly mean precipitation anomalies from 1979 to 2007 was performed to extract the first three EOF modes of interannual variability in the subtropical and midlatitude EA monsoon domain (20°–50°N, 100°–130°E). The domain did not extend eastward beyond 130°E, because a large portion of the precipitation beyond 130°E comes from tropical cyclones, which might be influenced by factors different from those that normally govern EA monsoon variability.

We focused on the first three MJ and JA modes because these modes explain 60% and 65% of total MJ and JA variances, respectively. These principal modes are considered to be more predictable than other higher modes. For convenience of discussion, we will refer the first EOF mode in MJ to as MJ-1. Similar abbreviations apply to MJ-2, MJ-3, and all JA modes.

3. Subdivision of the East Asian summer monsoon

In this section, we first elaborate on why we think the EA summer monsoon can be divided into two subseasons, early (MJ) and late (JA) summer; we then contrast the differences in mean state between early and late summer. The latter provides background information for understanding how the basic state regulates the interannual response of the EASM to lower boundary forcing.

Figure 1 shows the seasonal march of the climatological monthly mean rainfall pattern from May to August. It is evident that the seasonal march from June to July is notably abrupt, whereas changes from May to

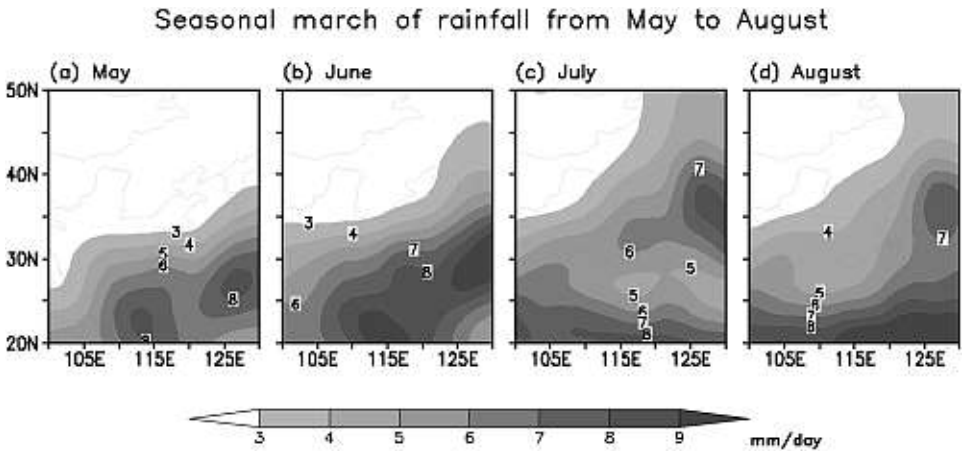

FIG. 1. Climatological monthly mean precipitation rate (in units of mm day^{-1}): (a) May, (b) June, (c) July, and (d) August. The precipitation data used are derived from CMAP for the period of 1979–2007.

June and from July to August are both relatively gradual. In May and June, the major rainy regions are similar and are confined to southern China except for a slight northward advance and an enhancement of the subtropical frontal rainfall (Figs. 1a,b). From June to July, however, the rainfall distribution changes abruptly: the well-known midsummer dry spell starts in southern China; meanwhile, the subtropical rainy zone shifts northward to north of Yangtze River, and the rainfall center along 125°E jumps from 29°N to 35°N (Figs. 1b,c). The change from July and August is also gradual (Figs. 1c,d). Therefore, there is a climatological basis to divide the EA summer into early summer (MJ) and late summer (JA).

Figure 2 maps the difference between the MJ and JA mean precipitation rates (JA minus MJ). In comparison with the rainfall distribution shown in Fig. 1, the negative rainfall area in Fig. 2 coincides with the major location of the maximum MJ rainfall, while the positive rainfall region indicates the location of the maximum JA subtropical rainfall. Given this pronounced change in precipitation, the circulation fields are expected to also undergo notable changes from early to late summer.

Figure 3 presents the mean monsoon circulation averaged for MJ and JA along with the bimonthly mean rainfall rate. Figure 3 confirms that the rainy region is primarily located in southern China (south of 32°N) and Okinawa, Japan, in MJ, while the major rainy region moves to the Korean Peninsula and northern China during JA. How do the large-scale processes determine MJ and JA precipitation over the EA subtropical and extratropical regions? We note that the MJ and JA precipitation distributions are determined primarily by the seasonal advance of the western North Pacific (WNP) subtropical high. At the longitude of 125°E, the WNP subtropical high ridge is located around 19°N in MJ, while it moves to about 28°N in JA. Meanwhile, the western periphery of the WNP subtropical high (signified by the contour of 1540 m) retreats eastward from 125°E in MJ to 135°E in JA. Note also that, in the tropics, the precipitation distribution is determined by the WNP monsoon trough over the Philippine Sea. The WNP monsoon trough is absent in the MJ period and well established in JA. In summary, the MJ and JA mean states are remarkably different.

4. Distinctions between principal modes of MJ and JA interannual variability

Figure 4 compares the spatial patterns and corresponding principal components (PCs) of interannual

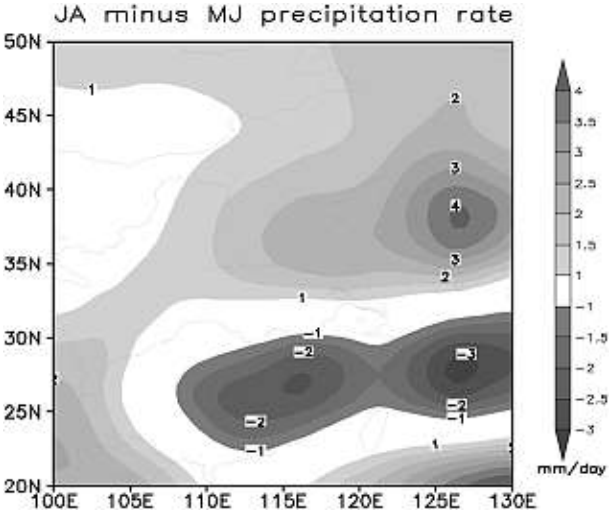

FIG. 2. Difference in climatological mean precipitation rate between late (JA) and early (MJ) summer: JA minus MJ.

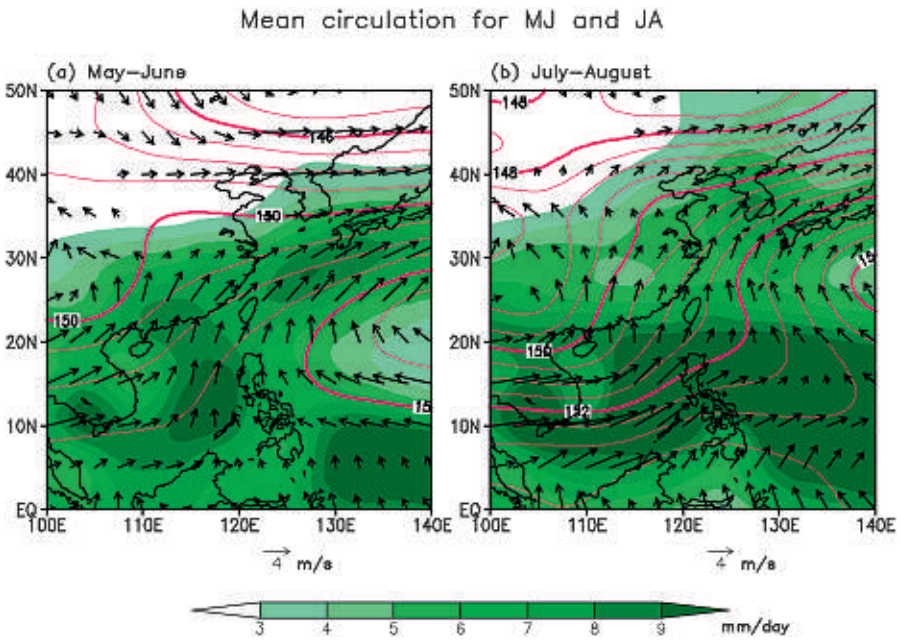

FIG. 3. Climatological mean 850-hPa winds (arrows in units of m s^{-1}), geopotential height (contours in units of 10 gpm), and precipitation rate (color shading in units of mm day^{-1}) averaged for (a) May–June and (b) July–August. The circulation data used are derived from NCEP reanalysis 2. The precipitation data used are derived from CMAP.

variation between the MJ and JA rainfall anomalies. Figure 4a shows that the central segment of the rain belt associated with MJ-1, MJ-2, and MJ-3 modes shifts systematically northward from 23° to 33°N, and the western edge of the anomalous rainband shifts eastward from 106° to 114°E. Figure 4b shows three leading JA modes. The JA-1 and JA-3 patterns show a northward movement of the EASM rain belt. The pattern of the second mode (JA-2) is totally different from JA-1 and JA-3 and features a dipole pattern with one pole near Hainan Island and the major pole over central Okinawa. Note that the three MJ modes and three JA modes signify different anomaly patterns. The dissimilar spatial patterns suggest that the MJ and JA anomalies may be better predicted separately.

Why do the MJ and JA modes have unlike spatial structures? Fig. 3 shows the mean position of the rainbands in MJ and JA, and these positions are significantly different. In MJ, the normal subtropical rain belt is located from south of the Yangtze River to Okinawa (Fig. 3a). Thus, MJ-1 and MJ-3 represent, respectively, a southwestward and northeastward shift of the normal rain belt, while the MJ-2 pattern implies an enhanced climatological rain belt (Fig. 4a). In JA, the climatological position of the rain belt is located in the Yellow River valley; thus, the JA-1 pattern implies a southward shift of the normal rain belt, while the JA-3 pattern means that the rain belt is enhanced in the normal location and extended northward to Mongolia. In summary, the enhanced rainfalls of the three EOF modes of MJ anomalies are basically collocated with the MJ mean position of the rainband, while the enhanced rainfalls of the three JA modes are also mainly collocated with the JA mean rainfall region. This linkage suggests that the interannual anomalies are likely modulated by the seasonal march of the EA subtropical front.

Not only are the spatial patterns dissimilar, but the temporal evolution of the PCs of the MJ and JA modes also shows notable differences. The PCs of all three MJ modes tend to exhibit a decadal modulation of interannual variation. The MJ-1 mode seems to be inactive in the 1980s but amplified after the mid-1990s (Fig. 2a). The MJ-2 mode shows the opposite tendency (lower-middle panel, Fig. 2a). The MJ-3 mode has a regular 5-yr oscillation before the late 1990s but becomes inactive afterward (lower-right panel, Fig. 2a). These results seem to suggest that the MJ modes might have experienced a decadal change around the mid–late 1990s. Kwon et al. (2005) have detected a sudden change in precipitation and circulation in Southeast Asia and the Philippines around the mid-1990s during the recent period after 1979. The topic of whether the change in behavior of the three MJ modes is related to the decadal change documented by Kwon et al. deserves further investigation. In contrast, the principal components of the three JA modes have little decadal modulation

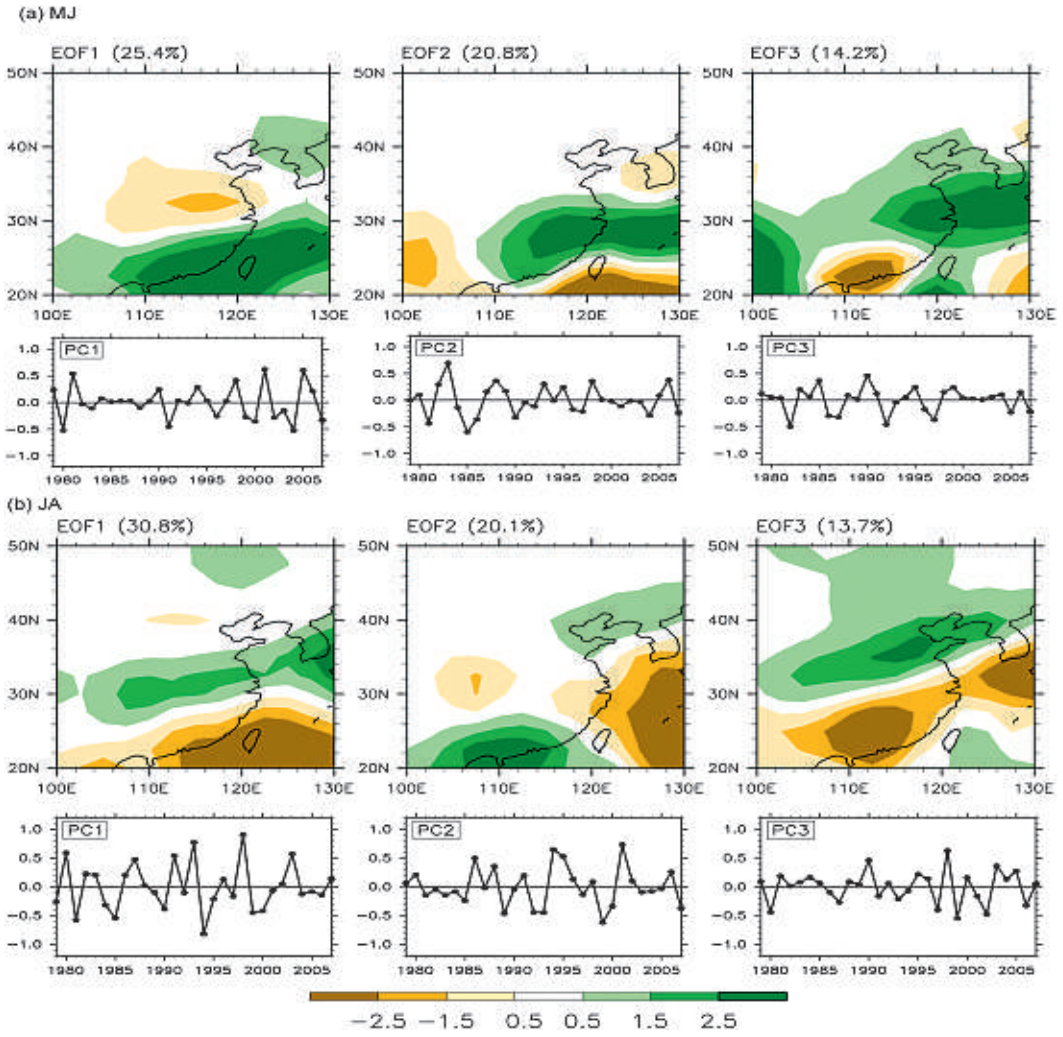

FIG. 4. Comparison of the first three leading modes of interannual variation for (a) MJ and (b) JA, derived for the period of 1979–2007. The upper panels in (a) and (b) are spatial patterns of precipitation anomalies (colors in units of mm day^{-1}) and the lower panels are the corresponding PCs. The fractional variance is shown at the top of each panel for each mode.

except in JA-3. It is also conceivable that the origins of the MJ and JA modes might differ to some extent.

5. ENSO-related and non-ENSO-related principal modes

In terms of the origins, we found *two categories of modes*: ENSO related and non-ENSO related. This can be seen from Fig. 5, which presents lead–lag correlation coefficients between the equatorial Indo-Pacific SST anomalies and each principal component associated with the major MJ and JA modes. The MJ-1 mode has no significant relationship with the equatorial eastern and central Pacific SST anomalies. The JA-2 mode is also unrelated to ENSO because no signal exists in the equatorial eastern Pacific. These two modes may be considered non-ENSO-related modes. The other four remaining modes all have significant, simultaneous, or lead–lag correlations with the equatorial eastern Pacific SST anomalies within ±6 months; they are considered ENSO-related modes.

Quantitatively, the ENSO-related MJ modes (MJ-2 and MJ-3) contribute 35% of the total MJ variance, while the ENSO-related JA modes (JA-1 and JA-3) account for 45% of the total JA variance. Therefore, JA anomalies seem to have a closer link with ENSO than MJ anomalies. We also note that the non-ENSO modes contribute considerably to MJ and JA variances. MJ-1 accounts for 25% of the total MJ variance, which amounts to 70% of the corresponding ENSO-related

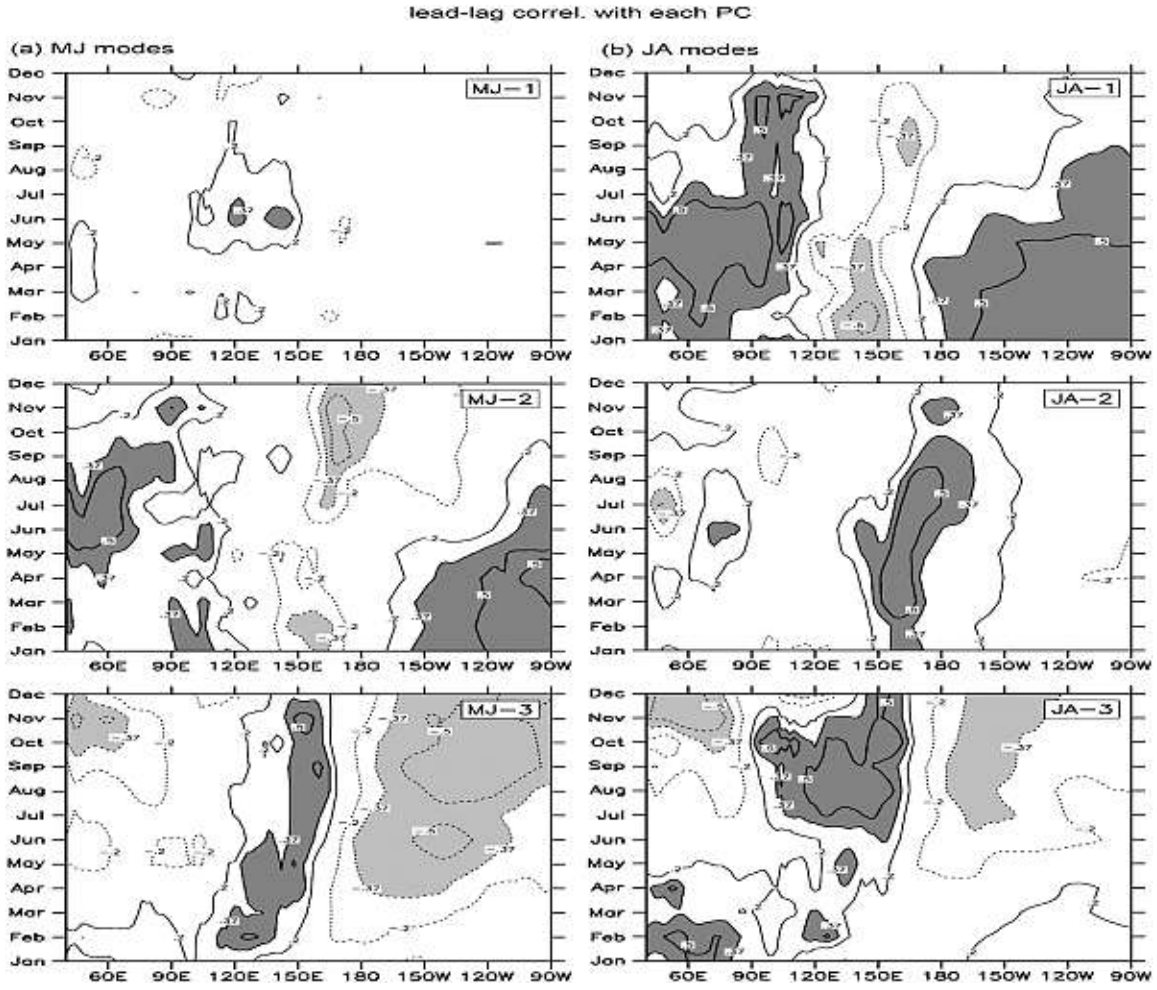

FIG. 5. Relationships between the MJ and JA principal modes and the equatorial Indian–Pacific (40°E–90°W) SST anomalies averaged between 10°S and 10°N. The relationships are shown by the lead–lag correlation coefficients of three-month running mean SST anomalies with reference to each PC of (a) MJ-1, MJ-2, and MJ-3; and (b) JA-1, JA-2, and JA-3. The shaded areas represent the correlation coefficients significant at the 95% confidence level.

variability, and JA-2 contributes 20% of the JA variance, about half of the contribution of the ENSO-related modes. Therefore, understanding these non-ENSO sources of variability is necessary, especially during ENSO neutral years when they may become major sources of variability. Uncovering the sources of variability for these non-ENSO-related modes is challenging but essential for seasonal prediction in the absence of ENSO anomalies.

It is noted that the ENSO-related variations in both MJ and JA depend on the phases of ENSO. Figure 6 shows the bimonthly SST anomalies associated with each ENSO-related mode from January–February to September–October. Clearly, the MJ-2 and JA-1 modes occur in the decaying summer of an El Niño event. On the other hand, the MJ-3 and JA-3 modes concur with the development of a La Niña event. Keep in mind that if a spatial pattern is associated with El Niño, then the pattern with opposite polarities can be interpreted as associated with La Niña or vice versa. While MJ-2 and JA-1 modes generally occur in the decaying summer of El Niño or La Niña (Fig. 6), as far as individual years are concerned, there are exceptions. For example, based on the principal component shown in Fig. 4, the MJ-2 mode has large amplitude in 2006 and 2007 (Fig. 4a), but these are not years of a decaying summer of ENSO. For the JA-1 mode, 1991 is an exception (Fig. 4b). Similarly, while the MJ-3 and JA-3 modes generally occur during the development of La Niña (El Niño) events, 1985 and 1992 are exceptions (Fig. 4b).

Note also that, from the fractional variance of the ENSO-related modes, one may find that the MJ-2 and JA-1 modes account for about two-thirds of the total ENSO-related variance, suggesting that about two-thirds

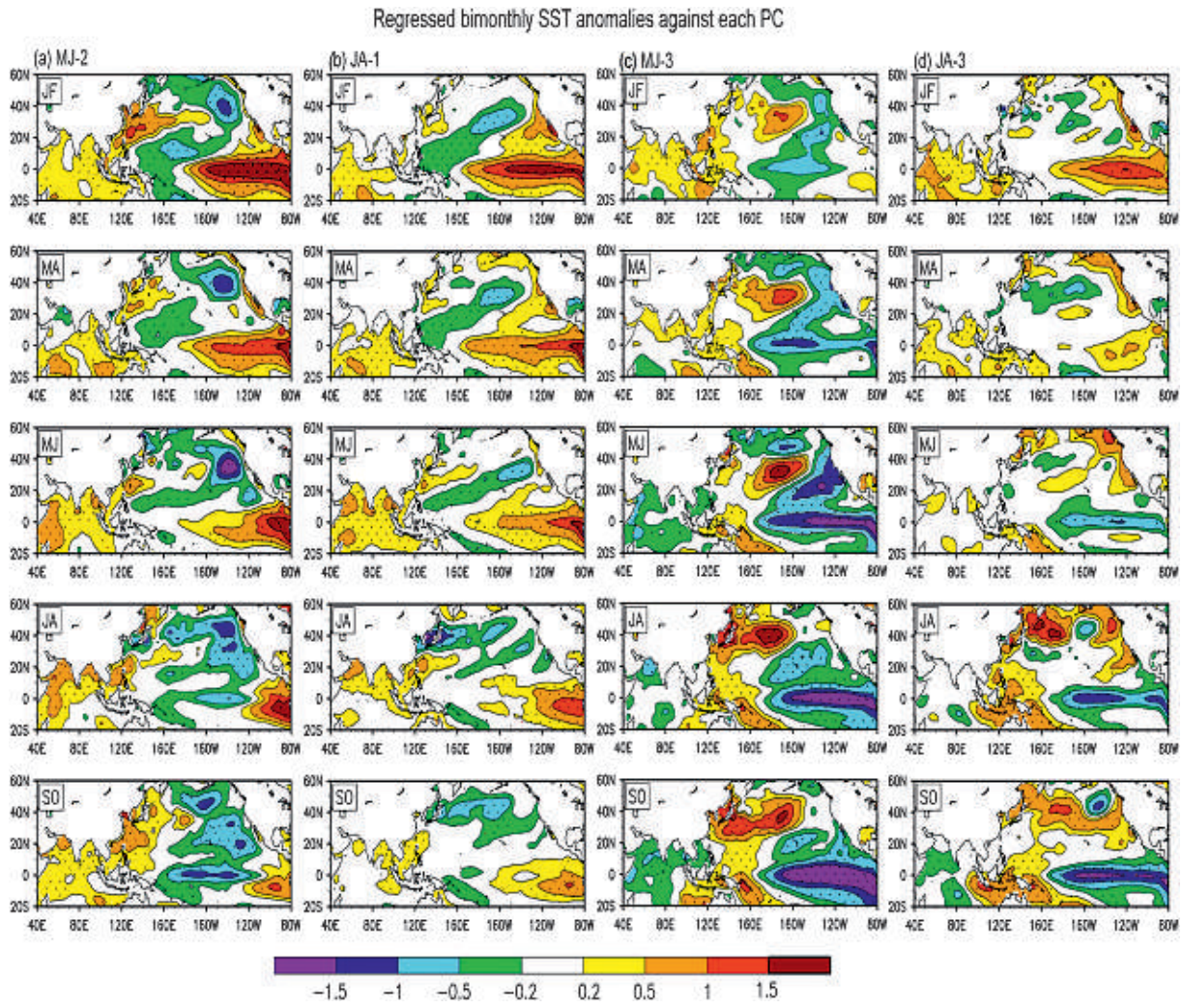

FIG. 6. Bimonthly SST anomalies (in units of K) regressed with reference to the corresponding PCs from January–February (JF) through September–October (SO) for the ENSO-related MJ and JA modes: (a) MJ-2, (b) JA-1, (c) MJ-3, and (d) JA-3.

of ENSO-related variance occurs during the decaying phase of ENSO, while only one-third of ENSO-related variance is associated with a developing ENSO phase.

6. What causes the differences between the ENSO-related MJ and JA modes?

As shown in Fig. 4, the ENSO-related MJ and JA modes have different spatial structures. How can the anomalous response to ENSO be quite different during the MJ and JA periods? There are two major reasons. First, the timing of ENSO development and decay is different. Second, the mean states of MJ and JA are remarkably different, as shown in Fig. 3, which may affect the response of the EASM to ENSO.

a. Different ENSO evolution associated with ENSO-related MJ and JA modes

Although both MJ-2 and JA-1 are associated with decaying El Niño events, the corresponding ENSO evolutions differ. MJ-2 is associated with a rapid decay of a strong El Niño, because by July the central-eastern Pacific positive SST anomaly almost disappears (Fig. 6a). On the other hand, JA-1 is associated with a slow decay, because a significant SST anomaly in the central-eastern Pacific remains during JA (Fig. 6b). Likewise, MJ-3 is associated with early development of La Niña; namely, the eastern-central Pacific cooling is well underway in March and April (Fig. 6c). Conversely, JA-3 is associated with late development of La Niña; that is, March and April is a transition period, and a cold anomaly does not occur over the eastern Pacific until May and June (Fig. 6d).

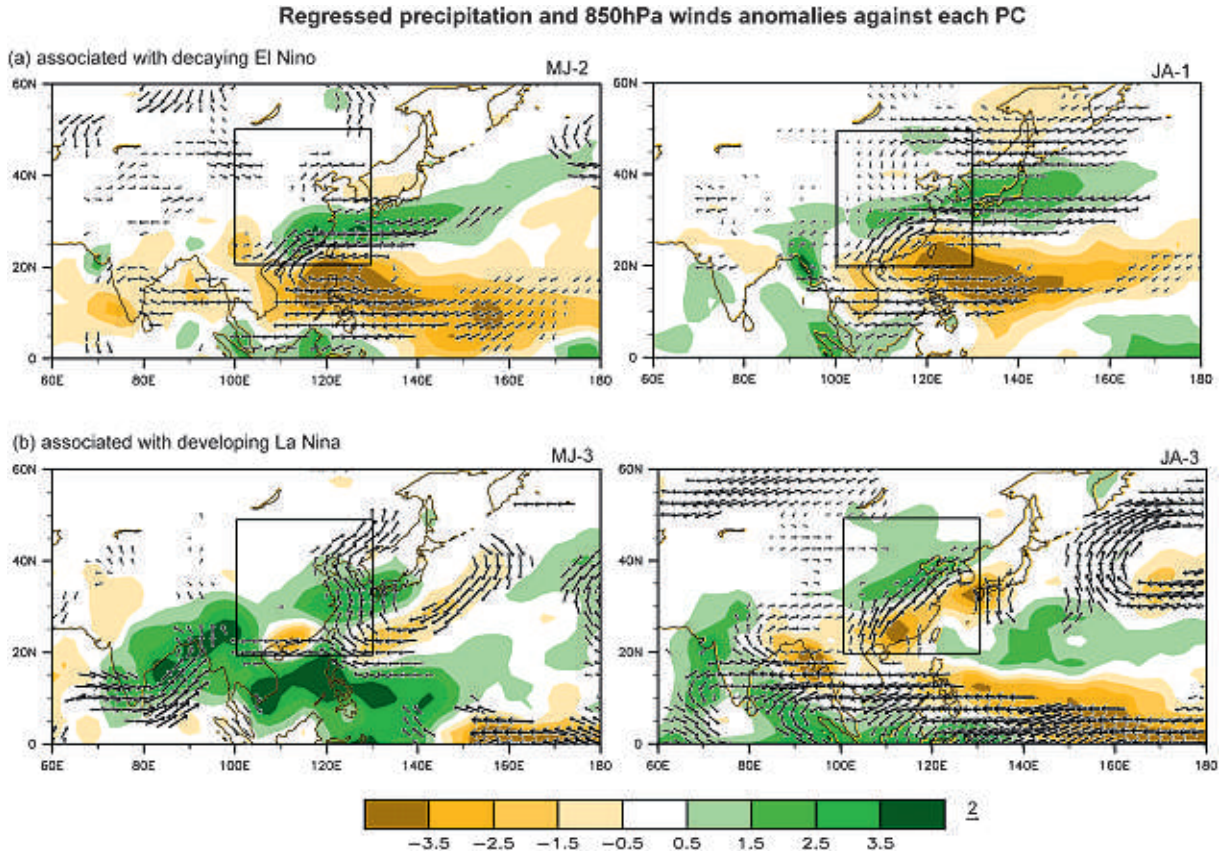

FIG. 7. Regressed anomalous precipitation (colors in units of mm day^{-1}) and 850-hPa anomalous winds (m s^{-1}) associated with (a) decaying El Niño (MJ-2 and JA-1 modes) and (b) developing La Niña (MJ-3 and JA-3 modes). The regression was made with reference to the corresponding PC. Wind vectors that are not statistically significant at the 95% confidence level were omitted. The EASM domain used for the EOF analysis (20°–50°N, 100°–130°E) is also outlined in each panel.

Note that while the ENSO-related MJ modes generally concur with rapid decay or early development of ENSO episodes, and the opposite tends to apply to ENSO-related JA modes (Fig. 6), close examination of the PC shown in Fig. 4 suggests that not all of the developing and decaying ENSO years show distinctions between the MJ and JA ENSO-related modes. For instance, the 1997/98 event is an exception: both MJ-3 and JA-3 have a negative PC value in 1997, and both MJ-2 and JA-1 have a positive PC value in 1998, suggesting that the MJ and JA ENSO-related modes are not distinctive.

Why does the slow decay of El Niño favor the JA-1 mode? During a decaying El Niño, the Philippine Sea anomalous anticyclone (PSAC; Fig. 7a) is the critical system that conveys delayed El Niño impact to the EASM (Wang et al. 2000; Chang et al. 2000). If the PSAC remains longer, it will affect JA rainfall; otherwise, it affects only MJ. Although the PSAC is primarily maintained by local air–sea interaction in the WNP warm pool from the spring to the subsequent summer (Wang et al. 2000; Lau et al. 2004), if the eastern Pacific SST anomaly lasts longer (in a low-frequency ENSO, for instance), its remote forcing additionally contributes to the persistence of the PSAC (Wang et al. 2000), favoring prolonged impact on the EASM.

b. Influence of the mean states on the EASM response to ENSO

How does the mean state modify the response to ENSO forcing? ENSO affects the EASM by modifying the location and strength of the WNP monsoon trough and WNP subtropical high. In MJ, the ENSO impacts the EASM primarily through displacement of the WNP subtropical high, which influences the subtropical frontal precipitation (Chang et al. 2000; Wang et al. 2000). On the other hand, in JA, ENSO impacts the EASM by changing the strength of the WNP monsoon trough convection over the Philippine Sea, which indirectly affects the WNP subtropical high and the subtropical frontal rainfall north of the WNP subtropical high through a meridional teleconnection, the

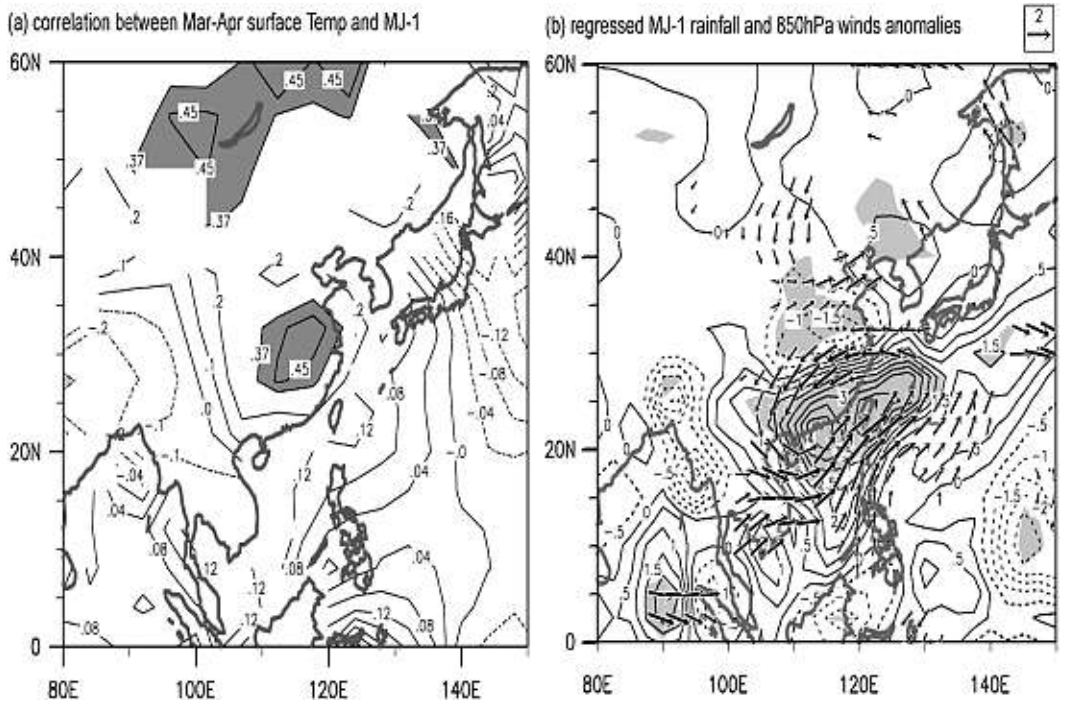

FIG. 8. (a) Correlation coefficient maps between the PC MJ-1 and the previous March–April mean land surface temperature and SST anomalies. (b) Regressed precipitation and 850-hPa wind anomalies with reference to the PC in MJ-1. The shaded areas indicate statistical significance at the 95% confidence level.

so-called Pacific–Japan pattern (Nitta 1987; Huang and Wu 1989).

As stated in section 4, the enhanced rainfall in the three EOF modes of MJ anomalies are basically collocated with the MJ mean position of the rainband, while the enhanced rainfall in the three JA modes are also mainly collocated with the JA mean rainfall region. During the decay of El Niño, rainfall increases along the anomalous rain belt from the lower reaches of the Yangtze River to Okinawa in MJ (left panel, Fig. 7a), but rainfall increases in the Huai River valley, South Korea, and Japan in JA (right panel, Fig. 7a). During the development of La Niña, MJ rainfall increases over the lower reaches of the Yangtze River and southern Japan (left panel, Fig. 7b), but JA rainfall increases over the lower reaches of the Yellow River valley and northern China–northern Korea and decreases in southern China and south Japan (right panel, Fig. 7b). Note that the subtropical front zone is a narrow band in a meridional direction. The rainfall anomalies in MJ-3 (Fig. 7b, left) coincide with a typical mei-yu/baiu, but the anomalous rainband in JA-3 (Fig. 7b, right) is located north of the traditional mei-yu/baiu band. The northward shift of the anomalous rainband in JA (by about 5° of latitude) is consistent with the corresponding northward shift of the WNP subtropical high ridge and tropical convective anomaly over the Philippines. The northward shift is consistent with the seasonal march of the tropical WNP monsoon trough, the WNP subtropical high, and the subtropical front. Similar discussion also applies to the difference between MJ-2 and JA-1 (Fig. 7a) in the decaying phase of ENSO.

7. Possible causes of non-ENSO modes

We found that the non-ENSO MJ-1 mode may be related to land surface anomalies in the preceding March and April. This is supported by the evidence shown in Fig. 8a. During March and April, significant land surface warming occurs in southeastern China. This warming area corresponds generally to a dry condition during the spring (figure not shown). In the subsequent MJ, a localized cyclonic anomaly develops downstream along the southeastern coast of China (Fig. 8b). This anomalous low-level circulation is quite localized, but it enhances the southeast China rainfall with concurrently suppressed rainfall to the north of the Yangtze River. We speculate that the March–April land surface warming in south China may induce the anomalous low pressure slightly downstream of the land warming area during MJ, forming the anomalous cyclone along the coast of southeastern China (Fig. 8b). Another region of notable

land surface warming in March and April is seen over Mongolia and Lake Baikal (Fig. 8a). Arai and Kimoto (2005) found that when the surface temperature over Siberia is high in April, the blocking events occur more frequently than normal over northeastern Siberia and the Okhotsk Sea in MJ. Associated with enhanced blocking activity, the surface Okhotsk high intensifies in MJ, affecting EA early summer precipitation. The impact of the notable springtime warming on EA early summer precipitation in the vicinity of Lake Baikal remains to be further studied. Chen and Yan (1981) showed that excessive snow cover on the Tibetan Plateau during winter/spring is associated with above-normal May–June rainfall in southern China. This finding needs to be verified with more reliable and updated data. Note also that Tibetan Plateau snow cover may not be an independent factor, as it is affected by ENSO (Wu and Kirtman 2007).

For the non-ENSO-related JA-2 mode, one of the precursors is persistent SST warm anomalies in the equatorial western Pacific between 150°E and the date line—the Niño-4 region (Fig. 5b). The significant positive anomaly between JA-2 and the equatorial western Pacific SST anomaly occurs as early as the previous January. The positive correlation further strengthens with time, and the region of positive correlation expands from March to June before JA (Fig. 5b). This signal may suggest a continuous increase in the equatorial western Pacific warming in the Niño-4 region prior to the JA season. How this affects East Asia remains elusive.

Further examination of the circulation anomaly associated with the JA-2 mode prior to JA may be helpful. It is seen that the tropical convergence zone in the Indo-Pacific sector in MJ is enhanced, and an anomalous WNP anticyclone is centered to the east of Okinawa (25°N, 130°E; Fig. 9a). From MJ to JA, there is a northward advance of the anomalous WNP anticyclone from Okinawa to the East China Sea (30°N, 130°E) at 850 hPa. This anomalous anticyclone has a barotropic structure with a slight northward tilt with height so that the center at 300 hPa is around 35°N, 130°E (Fig. 9b). We found that a wave train extends from central Asia (east of the Caspian Sea) to the North Pacific along a path that is similar to the circumglobal teleconnection route (Ding and Wang 2005). The wave train from central Asia to East Asia, called the ''Silk Road'' teleconnection by Enomoto et al. (2003), normally occurs in August. The strong anticyclonic anomaly center is located over the East China Sea, which induces suppressed rainfall in the East China Sea and south of Japan (Fig. 9b). The low pressure cell over southern China produces increased rainfall near Hainan Island (Fig. 9b). The Silk Road teleconnection is a mechanism through which enhanced rainfall over northern India and Pakistan (and thus, an enhanced central Asian anomalous high) may induce a high anomaly over northeastern Asia and affect Japan and northern China rainfall during JA (Ding and Wang 2005). The teleconnection pattern shown in Fig. 9b is similar to the Silk Road teleconnection, except that the action centers tend to be slightly south of it. Therefore, JA-2 may be related to a strong northern Indian monsoon, which may occur without ENSO impact (Ding and Wang 2005).

8. Summary and discussion

The major findings of this study are summarized as follows. First, we showed that the EA summer monsoon may be reasonably divided into early summer [May–June (MJ)] and late summer [July–August (JA)] because of rapid seasonal transition from June to July and that there exist remarkable differences in mean state between MJ and JA (Figs. 1–3). We also uncovered that the principal modes of interannual variation for early and late summer have distinctive spatial structure and temporal variability on a decadal time scale. Second, these principal modes can be classified as ENSO related and non-ENSO related. The former accounts for about 40%, while the latter accounts for about 23% of the total variance during 1979–2007; together, they may represent the predictable part of interannual variability. Third, we have shown that two-thirds (one-third) of the ENSO-related variances are associated with decaying (developing) phase of ENSO, and the difference between the ENSO-related MJ and JA modes lies in the timing (calendar months) when ENSO starts to decay or develop. Fourth, we have explored the origins of the non-ENSO-related modes. We have shown that the non-ENSO MJ mode is preceded by anomalous land surface temperatures over southern China during March and April. The non-ENSO JA mode links to the enduring equatorial western Pacific warming from the previous winter through late summer, and the enhanced rainfall over the northern Indian monsoon region may link to the northern China rainfall anomalies through the so-called Silk Road teleconnection (Enomoto et al. 2003) or a part of the circumglobal teleconnection pattern (Ding and Wang 2005). The physical mechanisms that establish these linkages deserve further investigation with numerical models.

The results of this study have important implications for the improvement of seasonal predictions of rainfall over East Asia. First, the current seasonal prediction focuses on JJA anomalies; however, the principal modes of JJA are similar to the corresponding primary

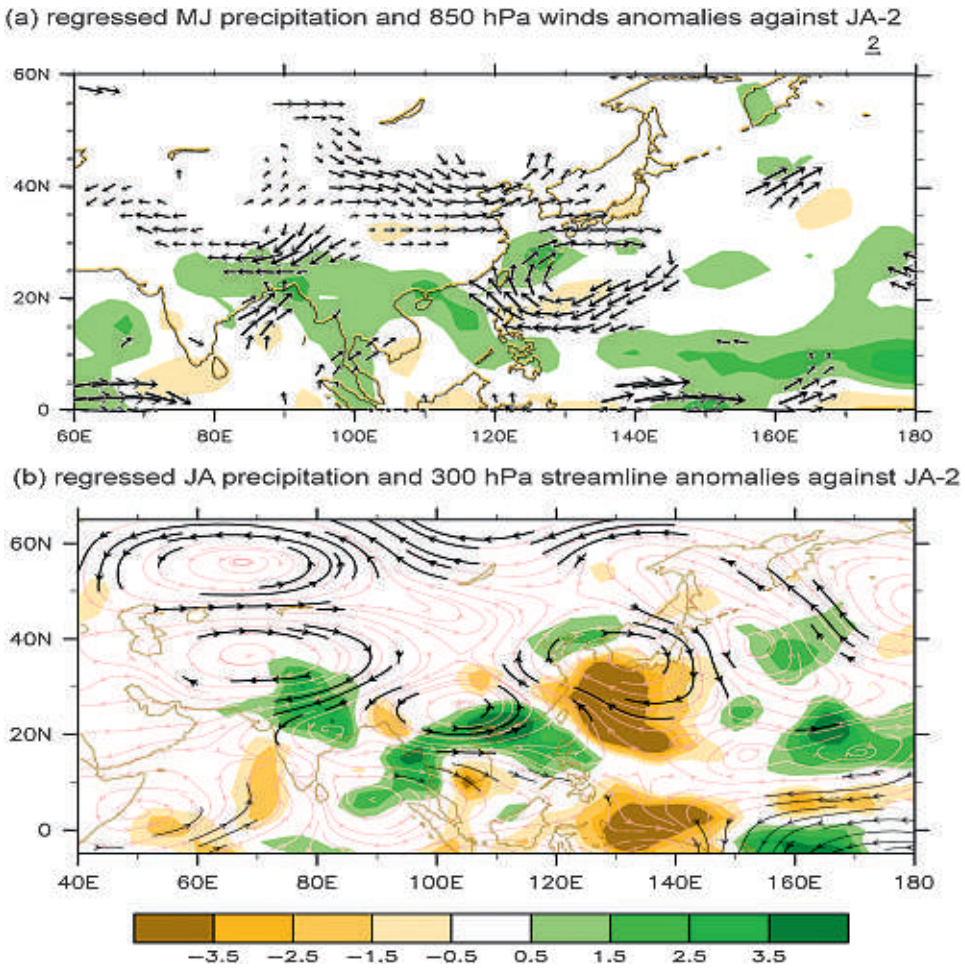

FIG. 9. Regressed May–June precipitation (colors in units of mm day^{-1}) and 850-hPa wind anomalies with reference to the PC of JA-2; (b) as in (a), but for July–August 300-hPa anomalous streamlines and precipitation anomalies. Shown are the wind anomalies that are statistically significant above the 95% confidence level.

modes of the JA anomalies (figure not shown). As such, the MJ anomalies may be underrepresented in a JJA forecast. Since the MJ and JA modes exhibit different spatial patterns (Fig. 4), separate prediction of the bimonthly (MJ and JA) anomalies may be useful. Another reason we recommend bimonthly prediction is because the intraseasonal oscillation may affect monthly prediction and make it less accurate. Two months is probably the shortest period required for linking statistical weather properties and anomalous lower boundary forcing. Second, the contribution of non-ENSO-related modes to the total variance is about 45%–70% of that of the ENSO-related modes; thus, the non-ENSO modes represent a significant potential source of predictability, especially during ENSO neutral years. Third, the ENSO-related modes depend on detailed ENSO evolutions, especially the timing of decay and development. Therefore, accurate prediction of the timing of ENSO decay and development is essential for prediction of EA summer rainfall.

The hypotheses concerning the origins of the non-ENSO modes, which are raised in this study, call for further numerical and theoretical studies. We have speculated that the non-ENSO JA-2 mode may provide additional predictability. This assertion is based on the linkage between JA-2 and Niño-4 SST anomalies and on the assumption that the Niño-4 SST anomalies are predictable. However, the JA-2 mode is also partially related to the non-ENSO-induced Indian monsoon variation. If JA-2 is dominantly determined by the latter, then it may not be predictable, because studies have shown that the atmospheric internal dynamics of the Indian summer monsoon's rainfall variability are quite strong, which may actually limit the seasonal prediction

of the Indian monsoon's rainfall (e.g., Goswami 1998; Goswami et al. 2006). The conclusions were derived based on the last 30 yr of data. Whether these conclusions change based on longer time scales is unknown and invites further investigation.

Acknowledgments. Bin Wang is supported by the NSF climate dynamics program (ATM06-29531) and in part by IPRC, which is in part sponsored by FRCGC/JAMSTEC, NASA, and NOAA. Jian Liu and Bin Wang acknowledge the financial support of the National Basic Research Program of China (Grant 2004CB720208) and the National Natural Science Foundation of China (Grants 40871007 and 40672210).

REFERENCES

Arai, M., and M. Kimoto, 2005: Relationship between springtime surface temperature and early summer blocking activity over Siberia. *J. Meteor. Soc. Japan,* **83,** 261–267.

Chang, C.-P., Y. Zhang, and T. Li, 2000: Interannual and interdecadal variations of the East Asian summer monsoon and tropical Pacific SSTs. Part I: Roles of the subtropical ridge. *J. Climate,* **13,** 4310–4325.

Chen, L. T., and Z. X. Yan, 1981: A statistical study of the impact of Himalayan winter-spring snow cover anomalies on the early summer monsoon (in Chinese). Collected papers on Medium- and Long-Term Hydrological and Meteorological Forecasts, Yangtze River Regulating Office, Ed., Vol. 2, Water Conservancy and Power Press, 133–141.

Ding, Q., and B. Wang, 2005: Circumglobal teleconnection in the Northern Hemisphere summer. *J. Climate,* **18,** 3483–3505.

Ding, Y., and D. R. Sikka, 2006: Synoptic systems and weather. *The Asian Monsoon,* B. Wang, Ed., Springer-Verlag, 131–201.

Enomoto, T., B. J. Hoskins, and Y. Matsuda, 2003: The formation mechanism of the Bonin high in August. *Quart. J. Roy. Meteor. Soc.,* **129,** 157–178.

Fu, C. B., and X. L. Teng, 1988: Relationship between summer climate in China and El Niño/southern oscillation phenomenon (in Chinese). *Chin. J. Atmos. Sci.,* **12** (Special Issue), 133–141.

Goswami, B. N., 1998: Interannual variations of Indian summer monsoon in a GCM: External conditions versus internal feedbacks. *J. Climate,* **11,** 501–522.

——, G. Wu, and T. Yasunari, 2006: Annual cycle, intraseasonal oscillations, and road-block to seasonal predictability of the Asian summer monsoon. *J. Climate,* **19,** 5078–5099.

Huang, R. H., and Y. F. Wu, 1989: The influence of ENSO on the summer climate of China and its mechanism. *Adv. Atmos. Sci.,* **6,** 21–32.

Jones, P. D., M. New, D. E. Parker, S. Martin, and I. G. Rigor, 1999: Surface air temperature and its variations over the last 150 years. *Rev. Geophys.,* **37,** 173–199.

Kanamitsu, M., W. Ebisuzaki, J. Woollen, S.-K. Yang, J. J. Sling, M. Fiorino, and G. L. Potter, 2002: NCEP–DOE AMIP-II Reanalysis (R-2). *Bull. Amer. Meteor. Soc.,* **83,** 1631–1643.

Kwon, M., J.-G. Jhun, B. Wang, S.-I. An, and J.-S. Kug, 2005: Decadal change in relationship between East Asian and WNP summer monsoons. *Geophys. Res. Lett.,* **32,** L16709, doi:10.1029/2005GL023026.

Lau, N.-C., and M. J. Nath, 2000: Impact of ENSO on the variability of the Asian–Australian monsoons as simulated in GCM experiments. *J. Climate,* **13,** 4287–4309.

——, ——, and H. Wang, 2004: Simulations by a GFDL GCM of ENSO-related variability of the coupled atmosphere-ocean system in the East Asian Monsoon region. *East Asian Monsoon,* C.-P. Chang, Ed., World Scientific Series on Meteorology of East Asia, Vol. 2, World Scientific, 271–300.

Matsumoto, J., and T. Murakami, 2002: Seasonal migration of monsoons between the northern and southern hemisphere as revealed from equatorially symmetric and asymmetric OLR data. *J. Meteor. Soc. Japan,* **80,** 419–437.

Nitta, T., 1987: Convective activities in the tropical western Pacific and their impact on the northern-hemisphere summer circulation. *J. Meteor. Soc. Japan,* **65,** 373–390.

Smith, T. M., and R. W. Reynolds, 2004: Improved Extended Reconstruction of SST (1854–1997). *J. Climate,* **17,** 2466–2477.

Tao, S., and L.-X. Chen, 1987: A review of recent research on the East Asian summer monsoon in China. *Monsoon Meteorology,* C.-P. Chang and T. N. Krishnamurti, Eds., Oxford University Press, 60–92.

Tu, C. W., 1955: China weather and world oscillations: Implications for long-term prediction of summer drought/flood (in Chinese). *Modern Sciences in China: Meteorology 1919–1949,* Scientific Press, 369–422.

Wang, B., and LinHo, 2002: Rainy season of the Asian–Pacific summer monsoon. *J. Climate,* **15,** 386–398.

——, R. Wu, and X. Fu, 2000: Pacific–East Asia teleconnection: How does ENSO affect East Asian climate? *J. Climate,* **13,** 1517–1536.

——, and Coauthors, 2008a: Advance and prospectus of seasonal prediction: Assessment of the APCC/CliPAS 14-model ensemble retrospective seasonal prediction (1980–2004). *Climate Dyn.,* **33,** 93–117, doi:10.1007/s00382-008-0460-0.

——, Z. Wu, J. Li, J. Liu, C.-P. Chang, Y. Ding, and G. Wu, 2008b: How to measure the strength of the East Asian summer monsoon? *J. Climate,* **21,** 4449–4463.

Wu, R., and B. P. Kirtman, 2007: Observed relationship of spring and summer East Asian rainfall with winter and spring Eurasian snow. *J. Climate,* **20,** 1285–1304.

Xie, P., and P. A. Arkin, 1997: Global precipitation: A 17-year monthly analysis based on gauge observations, satellite estimates and numerical model outputs. *Bull. Amer. Meteor. Soc.,* **78,** 2539–2558.

Xin, X., R. Yu, T. Zhou, and B. Wang, 2006: Drought in late spring of South China in recent decades. *J. Climate,* **19,** 3197–3206.

Yu, R., and T. Zhou, 2007: Seasonality and three-dimensional structure of the interdecadal change in East Asian monsoon. *J. Climate,* **20,** 5344–5355.